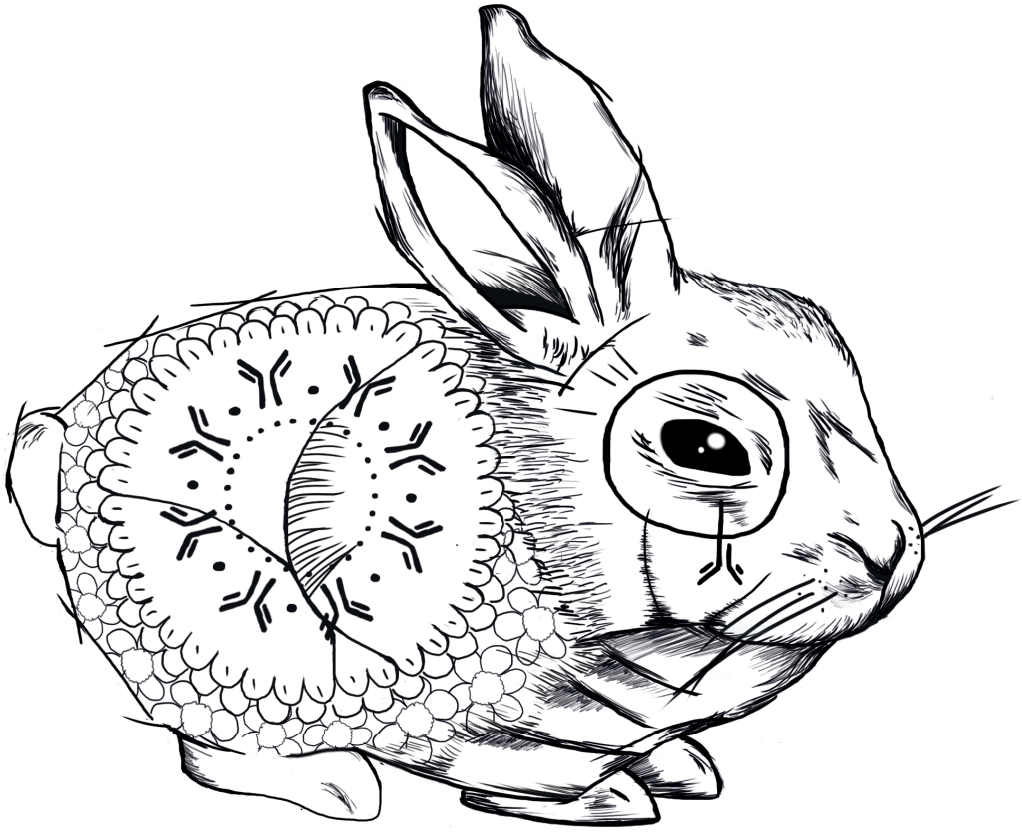

Chapter 4

Population Pharmacokinetics of Alemtuzumab (Campath) in Pediatric Hematopoietic Cell Transplantation: Towards Individualized Dosing to Improve Outcomes

Rick Admiraal
Cornelia M Jol-van der Zijde
Juliana M. Furtado Silva
Catherijne A.J. Knibbe
Arjan C. Lankester
Jaap J. Boelens
Geoff Hale
Annie Etuk
Melanie Wilson
Stuart Adams
Paul Veys
Charlotte van Kesteren
Robbert G.M. Bredius

Submitted

ABSTRACT

Introduction

Alemtuzumab (Campath®), a humanized anti-CD52 monoclonal antibody, is used to prevent graft-versus-host-disease and graft failure following pediatric hematopoietic cell transplantation (HCT). The therapeutic window is critical, with overexposure being associated with delayed immune reconstitution after HCT, potentially leading to viral reactivations and increased relapse chances. Individual exposure of alemtuzumab is unpredictable due to highly variable pharmacokinetics (PK). Therefore, patients treated with a comparable dose of alemtuzumab may have different drug exposure and thereby clinical outcomes. Describing the population pharmacokinetics in children is the first step towards evidence-based individualized dosing of alemtuzumab.

Methods

Serum alemtuzumab concentrations were measured in all children receiving a HCT with alemtuzumab as part of the conditioning regimen between January 2003 and July 2015, in two pediatric transplant centers. Population PK-analyses were performed using NONMEM 7.3.0. The current dosing regimen, a cumulative dose of 1 mg/kg, will be evaluated using simulation studies.

Results

A total of 1146 concentration samples from 206 patients were included, with age ranging from 2.4 months to 19 years old. Alemtuzumab PK could be best described using a 2-compartment model with parallel saturable and linear elimination pathways. Body weight was a predictor for central volume of distribution and clearance, a body weight dependent exponent was implemented in the latter. No relationships between baseline lymphocyte counts and pharmacokinetics were found. Simulations of the current dosing regimen showed an increase in exposure with increasing body weight.

Conclusion

The pharmacokinetics of alemtuzumab increase in a non-linear fashion with body weight. Therefore, any mg/kg-based dosing will lead to highly variable alemtuzumab exposure in children. Following determination of the therapeutic window, the proposed model can be used to develop an individualized dosing regimen for alemtuzumab, taking into account body weight. Individualized dosing of alemtuzumab may improve outcome following pediatric HCT.

INTRODUCTION

Allogeneic hematopoietic cell transplantation (HCT) is a potentially curative treatment option for children with a variety of underlying diseases including malignancies, immune deficiencies and bone marrow failure. While the success rates of this procedure in terms of survival have been improving in the last decades, treatment related mortality (TRM) and recurrence of disease remain to be significant hurdles. Approaches to reduce mortality are essential, including the prevention of graft-versus-host-disease (GvHD), which contributes to both short-term and long-term morbidity and mortality following HCT.

Alemtuzumab (Campath®, Genzyme, MA, USA), a humanized anti-CD52 monoclonal antibody, was introduced as serotherapy in HCT to prevent GvHD but also graft failure by in-vivo depletion of lymphocytes. Other drugs used as serotherapy include the polyclonal antibody anti-thymocyte globulin (ATG). The choice of serotherapy is dictated by center preferences, and previous treatment with ATG due to the potential development of anti-ATG-antibodies at second exposure. Inclusion of alemtuzumab in the conditioning regimen significantly reduces the incidence of both acute and chronic GvHD[1–3], for which an exposure-dependent relationship between alemtuzumab concentrations and occurrence of acute GvHD was reported[4]. On the other hand, higher doses of alemtuzumab have been associated with delayed immune reconstitution (IR) by excessive lymphodepletion[5,6]. IR, especially of T-cells, is dependent on peripheral expansion of graft-infused cells during the first months after HCT; depletion of these T-cells may leave patients with no or little IR. This could potentially lead to increased viral reactivations as well as less graft-versus-leukemia effect, thereby abrogating the beneficial effect on GvHD reduction. Despite a reduced incidence of GvHD, the absence of improvement in survival chances with the inclusion of alemtuzumab[1,2,4,6–9] may be due to absence of T-cell IR. Moreover, most studies report on adult populations; few studies investigate alemtuzumab in pediatric populations.

While evidence suggests a relationship between the use of alemtuzumab and clinical outcomes in adult populations, individual exposure of alemtuzumab is unpredictable due to highly variable pharmacokinetics (PK)[10–13]. As a consequence, patients treated with a comparable dose of alemtuzumab may have significant differences in drug exposure and thereby clinical outcome. Part of this variability in pharmacokinetics of alemtuzumab may be due to non-linearity in clearance[7,10], where elimation changes from a first-order to a zero-order process after complete binding of targets (e.g. CD52 presented on cells)[14,15]. In addition, only descriptive pharmacokinetics of alemtuzumab are available in pediatric populations, while variability in PK is often most substantial in children[16,17]. The variable PK and frequent associations with outcome underline the need for predictable exposure to antibodies

between patients[10,18–21]. In line, the importance of dose individualization and/or therapeutic drug monitoring (TDM) of monoclonal antibodies is increasingly recognized[22,23].

Therefore, there is a great need for a population PK-model for alemtuzumab in pediatric patients receiving a HCT, in order to understand and explain the variability in pharmacokinetics and also to be able to adjust dosing on an individual level aiming for optimal alemtuzumab exposure in the future. In the current study, we describe the population PK of alemtuzumab in children receiving an HCT as a first step to develop an individualized dosing regimen.

PATIENTS AND METHODS

Study Design and Patients

Patients receiving a HCT with alemtuzumab as part of the conditioning, treated at the pediatric wards of the Leiden University Medical Center (Leiden, the Netherlands; LUMC) and Great Ormond Street Hospital (London, United Kingdom; GOSH) between January 2003 and July 2015, were included. In case of multiple HCT's per patient, all transplantations were included. Patients using other serotherapy drugs (anti-thymocyte globulin; ATG) within the same conditioning regimen were excluded. Additionally, patients who received any type of serotherapy in a 3-month period before this HCT were excluded from this analysis. No restrictions were applied on the timing and dose of alemtuzumab, or any patient, disease or transplantation related factors. Data were collected and samples were taken after informed consent was given through the parents and/or the child in accordance with the declaration of Helsinki. Ethical committee approval was acquired through trial numbers P01.028 (Leiden) and V0904 (London).

Alemtuzumab (Campath, Genzyme, Cambridge, MA, USA) was given as an intravenous infusion, usually starting 6-8 days before HCT for 4-5 consecutive days. In London, alemtuzumab was the standard choice for serotherapy, in Leiden, it was reserved for patients with patients with inflammation (selected immune deficiencies) and myelodysplastic syndrome, and for a short period of time standard serotherapy. Patients with hemophagocytic lymphohistiocytosis (HLH) received alemtuzumab 15 days before transplantation. Although the dose of alemtuzumab varied, most patients were given a cumulative dose of 1 mg/kg (5 x 0.2mg/kg/day), with a substantial number of patients receiving alemtuzumab at a cumulative dose of 0.5 mg/kg at the treating physician's discretion. Few included patients received in vitro lymphodepletion of the graft by adding 20mg of alemtuzumab to the infusion bag containing the graft some hours before infusion of the graft, either following a course of alemtuzumab or without receiving prior serotherapy. Patients receiving alemtuzumab

following allergic reactions to ATG in the same conditioning were excluded from this analysis. Conditioning regimens were given according to (inter)national protocols. GvHD-prophylaxis consisted of cyclosporin A (controlled with therapeutic drug monitoring at trough levels of 150-250 µg/L) combined with either prednisolone (cord blood transplants), methotrexate (matched unrelated donor). Patients receiving an identical related donor transplantation or CD34 selected graft did not receive any additional GvHD prophylaxis. All patients received selective gut decontamination and were treated in positive pressure, particle free air-filtered isolation rooms.

Samples for pharmacokinetic measurements were taken before and after each infusion, followed by one sample weekly in the patients from Leiden until approximately +70 days after HCT, while in London, three samples were available per patient: on the day of HCT (day 0), and +14 and +28 days after HCT. The samples around infusion were taken at ±15 minutes before and after infusion, respectively, which in light of the long half-life of alemtuzumab can be seen as true trough and peak levels. Samples were prospectively collected and measured in batches.

Measurement of alemtuzumab concentration and anti-alemtuzumab antibodies

Q-FACS assay

The laboratory in London, measuring part of the London population, used a Q-FACS assay. Alemtuzumab levels were measured using quantitative flow cytometry assays (Q-FACS), in modifications of the method described[24]. In short, $1x10^6$ HUT-78 T-cells were incubated using fourfold dilutions of patients serum in PBS, followed by washing and incubation with conjugated secondary antibodies (Alexa Fluor 647 labeled goat-anti-human IgG [Life Technologies]). To construct a reference curve, HUT-cells were incubated with known amounts of alemtuzumab (range 10-0.01 µg/ml), containing 25% human serum. Cells were washed and MFI was measured on a FACS Calibur machine (Becton Dickinson Biosciences, Franklin Lakes, NJ, USA). The lower limit of detection for alemtuzumab in this assay was 0.1 µg/mL.

ELISA assay

All concentration samples from Leiden and part of the samples from London were measured in Leiden using an ELISA-based assay. Microtitre plates (Corning Corporation, Corning, NY, USA) were coated with CD52 anti-idiotype (Geoff Hale Developments, D003p56) diluted in PBS at a concentration of 0.5 µg/mL by incubating overnight at 4°C after blocking with 2% casein in PBS. Samples, controls and a diluted standard range of alemtuzumab (25 ng/mL-0.1 ng/mL), diluted in 10% pooled human serum) were applied and incubated for 1 hr at room temperature (RT). After washing, bound alemtuzumab was detected with biotin-

labeled NC [anti-idiotype antibody (Geoff Hale Developments, D003p95, 0.2 µg/mL), 1 hr at RT, followed by streptavidin poly-HRP (Sanquin, 8000145253, 2 µg/mL), 30 min. The lower limit of detection was 0.01 µg/mL.

In both assays alemtuzumab spiked sera were used as controls. The results of 146 samples tested with both ELISA NC anti-idiotype and Q-FACS were compared. For the correlation only samples with a measured alemtuzumab concentration >0.1 µg/mL in QFACS were used. The correlation between the two used assays was good (R^2 0.89).

Population Pharmacokinetic Analysis

For analysis of the PK-data, non-linear mixed effects modeling was employed using NONMEM 7.3.0 (Icon, Hanover, MD, USA). R version 3.2.3 and Pirana version 2.8.2 were used for preparation and visualization of data. First order conditional estimation (FOCE) with interaction was used throughout model development. Alemtuzumab concentrations were logarithmically transformed and simultaneously fitted. Samples that were reported to be below the limit of quantification (BLQ), which only occurred in the tail end of concentration, and were set at half the BLQ with subsequent samples being removed in accordance with method M6[26]. Inter-individual variability on PK-parameters was assumed to follow a log-normal distribution, and were implemented in the model according to equation 1:

$$P_i = P_{pop} * e^{\eta_i} \quad \text{(Eq. 1)}$$

where P_i is the individual or post-hoc value of the parameter in the *i*th individual, P_{pop} is the population mean for this parameter, and η_i the inter-individual variability of the ith person, which samples from a normal distribution with a mean of 0 and a variance of ω^2. An additive error model was used, which due to logarithmically transformed data should be seen as a proportional error model. Here, the *j*th observation for the ith individual was described using equation 2:

$$Y_{i,j} = C_{pred,i,j} + \varepsilon \quad \text{(Eq. 2)}$$

where $Y_{i,j}$ is the observed concentration, $C_{pred,i,j}$ the jth predicted concentration for individual i, and ε the error, sampled from a normal distribution with a mean of 0 and a variance of σ^2.

Several criteria applied in the process of model building and selection. A decrease in objective function value (OFV) over 3.84 points between nested models was considered statistically significant, this correlated with $p<0.05$ based on a Chi-squared distribution with 1

degree of freedom. Goodness of fit plots were evaluated, including observed versus both individual and population predicted concentrations, as well as conditional weighted residuals (CWRES) versus time and observed concentrations. Additionally, parameter uncertainty and η-shrinkage were evaluated to assess model performance.

Inter-occasion variability (IOV) was tested to assess changes in parameters between the respective doses according to equation 3:

$$P_i = P_{pop} * e^{\eta_i + \kappa_m} \quad \text{(Eq. 3)}$$

where, compared to equation 1, κ_i is the inter-occasion variability for the *m*th occasion. Individual pharmacokinetic parameters (post-hocs) were estimated using the POSTHOC option in NONMEM

The elimination of antibodies is often dependent on the concentration of substrate[32,33], therefore non-linear elimination pathways were explored. No data was available on target concentrations over time (i.e. CD52, or lymphocytes), therefore full TMDD-models as previously described were not persued[33,34]. Instead, non-linear elimination pathways were explored by incorporating clearance described by Michaelis-Menten kinetics:

$$V = \frac{V_{max} * C}{K_m + C} \quad \text{(Eq. 4)}$$

where V is the elimination rate, V_{max} the maximum elimination rate, C the concentration alemtuzumab, and K_m the Michaelis-Menten constant; the concentration at which 50% of maximum elimination rate is reached.

Covariate Model

Patient characteristics, including body-size parameters, and transplant- and disease specific variables were studied as a possible covariate for their relation with PK-parameters. In line with previous reports, the role of lymphocyte counts on alemtuzumab pharmacokinetics was also investigated, as CD52 is almost exclusively expressed on these cells. Cell counts drawn before the first infusion of alemtuzumab were available; the lymphocyte counts are greatly reduced after the first dose in most patients and were therefore not available. Therefore, we considered lymphocyte counts drawn within 48 hours before infusion of the first alemtuzumab dose as a covariate.

To assess the covariate relations, post-hocs, inter-individual variability and CWRES were plotted against covariates, both before and after inclusion of the covariates, to evaluate potential relationships. Lastly, only those covariates where a physiological or pharmacological mechanism could be hypothesized were included. Continuous covariates such as age and body weight were tested in a linear and power function (equations 5 and 6):

$$P_i = P_{pop} * (1 + \left(\frac{Cov_i}{Cov_{median}}\right) * l) \quad \text{(Eq. 5)}$$

$$P_i = P_{pop} * \left(\frac{Cov_i}{Cov_{median}}\right)^k \quad \text{(Eq. 6)}$$

where P_i and Cov_i are the parameter and covariate value for the ith individual, P_{pop} the population mean for this parameter, Cov_{median} the standardized value for the covariate. In the linear relationship equation (eq. 5) l represents the slope factor of the linear function, while in the power-relationship equation (eq. 6) k is the scaling factor. Additionally, more complex variations of equation 6 were explored, where k is dependent on the covariate value of the ith individual, as proposed by Wang et al[27], and implemented in several other models[28,29]. Evaluated variations included an E_{max} approach and a power function according to:

$$k = k_0 - \frac{k_{max} * {BW_i}^{\Upsilon}}{{k_{50}}^{\Upsilon} + {BW_i}^{\Upsilon}} \quad \text{(Eq. 7)}$$

$$k = a * BW^b \quad \text{(Eq. 8)}$$

where k is the exponential scaling factor in equation 6, k_0 the value for the exponent for an individual with a hypothetical bodyweight of 0 kg, k_{max} the maximum decrease of the exponent, k_{50} the bodyweight at which 50% of k_{max} is reached, and Υ the hill coefficient determining the steepness of the sigmoidal decline. In a power function, a represents the coefficient and b is the exponent.

Potential covariates were evaluated using forward inclusion and backward elimination with a significance level of <0.005 (-7.9 points in OFV) and <0.001 (-10.8 points in OFV), respectively. Building of the covariate model was comparable to the development of the structural model. In addition, after inclusion of a covariate, a decline in unexplained inter-individual variability had to be achieved before inclusion into the final model[30].

Model Evaluation

As the main goal for this model is to guide future dosing in children, the model has to be thoroughly evaluated for its robustness. To assess the predictive performance of the model, bootstrap analyses were performed, stratified on treatment center. One thousand datasets were created using random selection from the original dataset; the final model was fit to each data set. For each parameter, median values from the thousand fits for each parameter as well as 95% confidence intervals were compared to parameter estimates of the final model.

In addition, a normalized prediction distribution of errors (NPDE) was performed, where the prediction discrepancies are simulated taking into account the correlation between observations in the same individual and the predictive distribution[31]. Finally, prediction-corrected visual predictive checks (VPC) were created to assess the predictive performance of the final model as compared to the measured concentrations.

Dose Simulations

To evaluate the current most frequently used dosing regimen for alemtuzumab (cumulative dose of 1 mg/kg over 5 days; 0.2 mg/kg/day), we performed simulation studies. Patients were selected based on representative covariate values; simulations were performed taking into account the full random effects model with 500 patients per group being simulated. Median as well as 95% confidence intervals of concentration over time are shown.

RESULTS

Patients

A total of 206 patients receiving 212 HCT's were included from the two treatment centers (Table 1). Median age was 4.8 years old, median body weight was 17.2 kilogram. Fifty-four percent of patients received a cumulative alemtuzumab dose of 0.9 to 1.1 mg/kg, while 35% received a cumulative dose of less than 0.9 mg/kg. Median starting day relative to the infusion of stem cells was -8 days, ranging from 0 days (alemtuzumab added to the bag containing the stem cells) to 21 days before transplantation. Most patients (52%) received a HCT to treat an immune deficiency; the most frequently used stem cell source was bone marrow. A total number of 1146 concentration samples were available for this analysis (median 5.4 samples per patient; Figure 1). The majority of the samples (84%, collected in 136 patients) were measured in Leiden.

Structural Pharmacokinetic Model

A two-compartment model best described the pharmacokinetics of alemtuzumab (Table 2; Figure 2). Compared to a one-compartment model, the two-compartment was superior in

terms of goodness-of-fit (GOF) plots and objective function value (253 points decrease in OFV; p<0.001). Three patients in the lowest body-weight group were significantly under-predicted in low concentrations (Figure S2). However, large residual standard errors in the parameters associated with distribution were observed, as well a high dependency on initial values. To address this issue, model simplification was applied with peripheral volume of

	London	Leiden	Total
Number of patients (n)	139	67	206
Number of HCTs (n)	139	73	212
Male sex (%)	66	67	67
Age (years)	4.0 (0.4-15)	7.3 (0.2-19)	4.8 (0.2-19)
Weight (kg)	16.0 (4.0-60)	21.0 (2.6-80)	17.2 (2.6-80)
Number of samples [n (mean per patient)]	343 (2.5)	803 (11.0)	1146 (5.4)
Location of Concentration Measurements (% of samples)			
Leiden	47	100	84
London	52	0	16
Starting day alemtuzumab (days before transplantation)	8 (5-21)	6 (0-16)	8 (0-21)
Lymphocyte count before conditioning (x 10^9)	0.74 (0.00-9.3)	0.54 (0.03-7.5)	0.74 (0.00-9.3)
Cumulative dose (mg/kg) [%]			
<0.9 mg/kg	37	31	35
0.9-1.1 mg/kg	50	62	54
>1.1 mg/kg	13	7	11
Diagnosis (%)			
Hematologic Malignancy	17	40	25
Immune deficiency	62	34	52
Bone marrow failure	15	25	18
Metabolic disease	5	0	4
Benign hematology	1	1	1
Stem cell source (%)			
Bone marrow	61	60	61
Peripheral blood stem cells	39	32	36
Cordblood	0	8	3
Conditioning regimen (%)			
Reduced intensity (NMA)	43	66	51
Chemotherapy-based (MA)	51	29	43
TBI-based (MA)	6	5	6

Shown as median (range) unless otherwise specified

Table 1. Patient Characteristics. HCT: hematopoietic cell transplantation; TBI: total body irradiation; NMA: non-myeloablative; MA: myeloablative

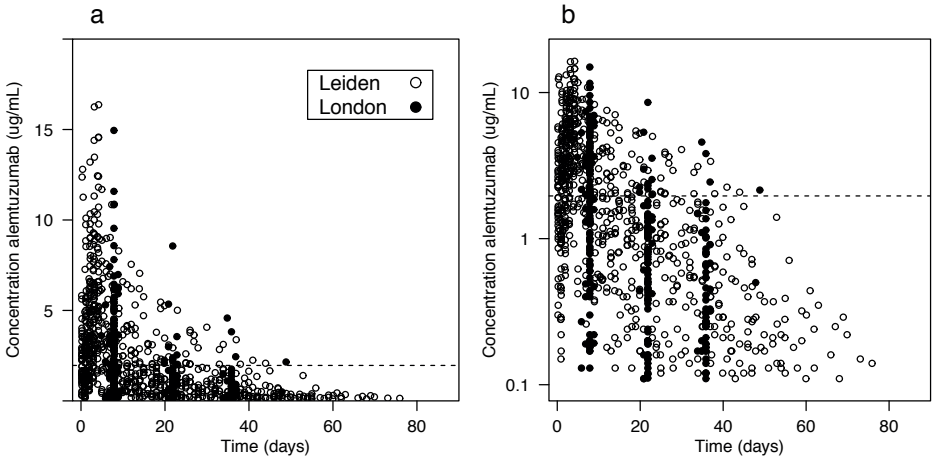

Figure 1. Concentration-time plots of all patients from LUMC Leiden (open circles) and GOSH London (dots) on a normal scale (panel a) and a log scale (panel b). Dashed line: Michaelis-Menten constant K_m.

	Dataset [estimate (RSE)]	Shrinkage (%)	1000 bootstrap replicates (99.1% successful)	
Parameter			Median	95% confidence interval
Structural model				
$Cl_i = CL_{pop} * \left(\frac{WT}{WT_{med}}\right)^{(a*WT)^b}$				
CL_{pop} (L/day)	0.20 (27%)		0.21	0.12-0.33
a	0.048 (33%)		0.047	0.022-0.102
b	-0.47 (30%)		-0.55	-2.53 - -0.2
$V_{1,i} = V_{1,pop} * \left(\frac{WT}{WT_{med}}\right)^{c}$				
$V_{1,pop}$ (L)	1.89 (9%)		1.87	1.49-2.3
c	0.72 (11%)		0.72	0.56-0.91
$V_{2,pop}$ (factor of V1)	0.82 (20%)		0.89	0.59-1.24
Q_{pop} (L/day)	0.33 (28%)		0.34	0.21-0.98
$V_{max,pop}$ (mg /day)	0.60 (30%)		0.63	0.28-0.99
$K_{m,pop}$ (mg/L)	1.96 (36%)		1.87	0.97-4.1
Random variability				
Inter-individual variability on CL (%)	117 (14%)	17	117	92-145
Inter-individual variability on V_1 (%)	56 (11%)	22	58	45-70
Inter-individual variability on K_m (%)	144 (9%)	30	140	111-180
Proportional residual error (%)	34 (9%)	18	33	28-39

Table 2. Parameter Estimates and Bootstrap Results. *Cl* linear clearance, *WT* body weight (kg), WT_{median} median population body weight (17.3 kg). V_1 central volume of distribution, V_2 peripheral volume of distribution, *Q* intercompartmental clearance, V_{max} maximum transport rate for saturable clearance pathway, K_m Michaelis–Menten constant saturable distribution for saturable clearance pathway, RSE relative standard error

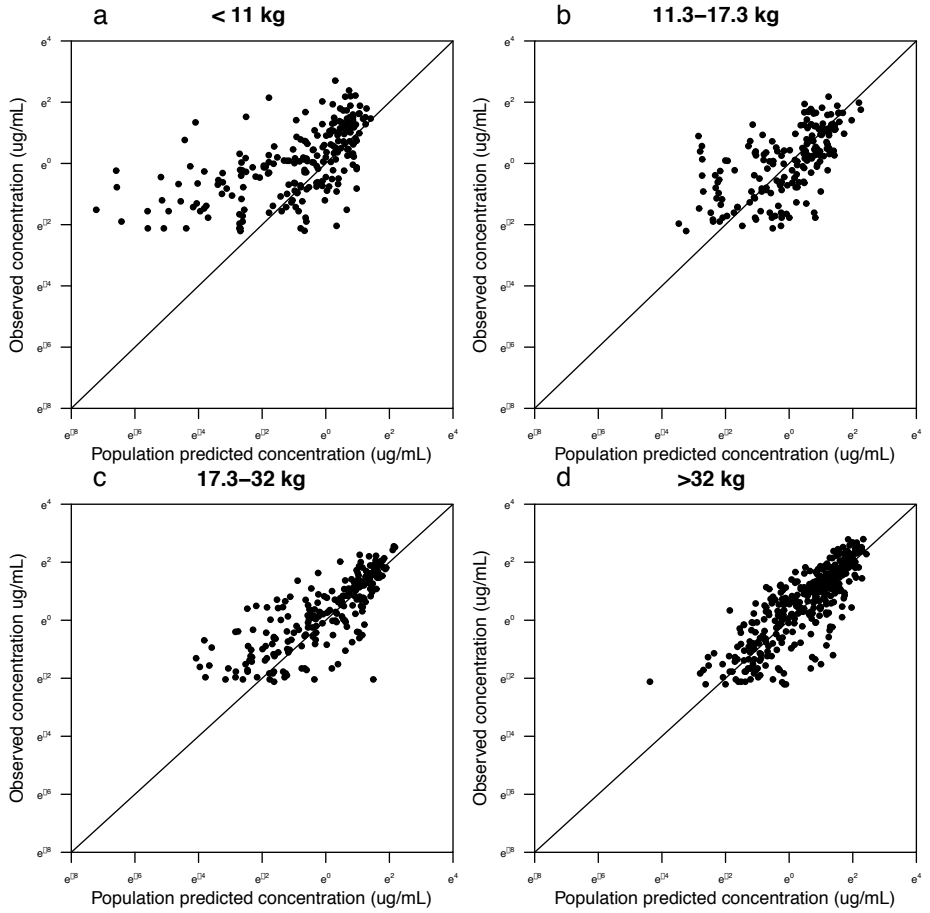

Figure 2. Goodness-of-fit plots of the final model: population predicted versus observed concentrations of alemtuzumab in all patients, split by quartiles of body weight. Panel A: < 11kg; Panel B: 11-17.3kg; Panel C: 17.3-32kg; Panel D: >32kg. Lines: line of unity (x=y). In the <11 kg group, three individuals are under-predicted.

distribution (V2) being estimated as a factor of central volume of distribution (V1), which made the model more stable and independent on initial values. This model yielded a decrease of 158 points in OFV compared to the one-compartment model ($p<0.001$), and showed comparable GOF plots compared to the full two-compartment model. A three-compartment model proved unstable, showing inaccurate parameter estimates. A proportional error model was incorporated in the model.

Looking at the individual concentration-time profiles, non-linear pharmacokinetics could be identified (Figure 1). Models with only non-linear clearance as well as models with parallel linear and non-linear clearance were evaluated. Here, compared to only linear clearance,

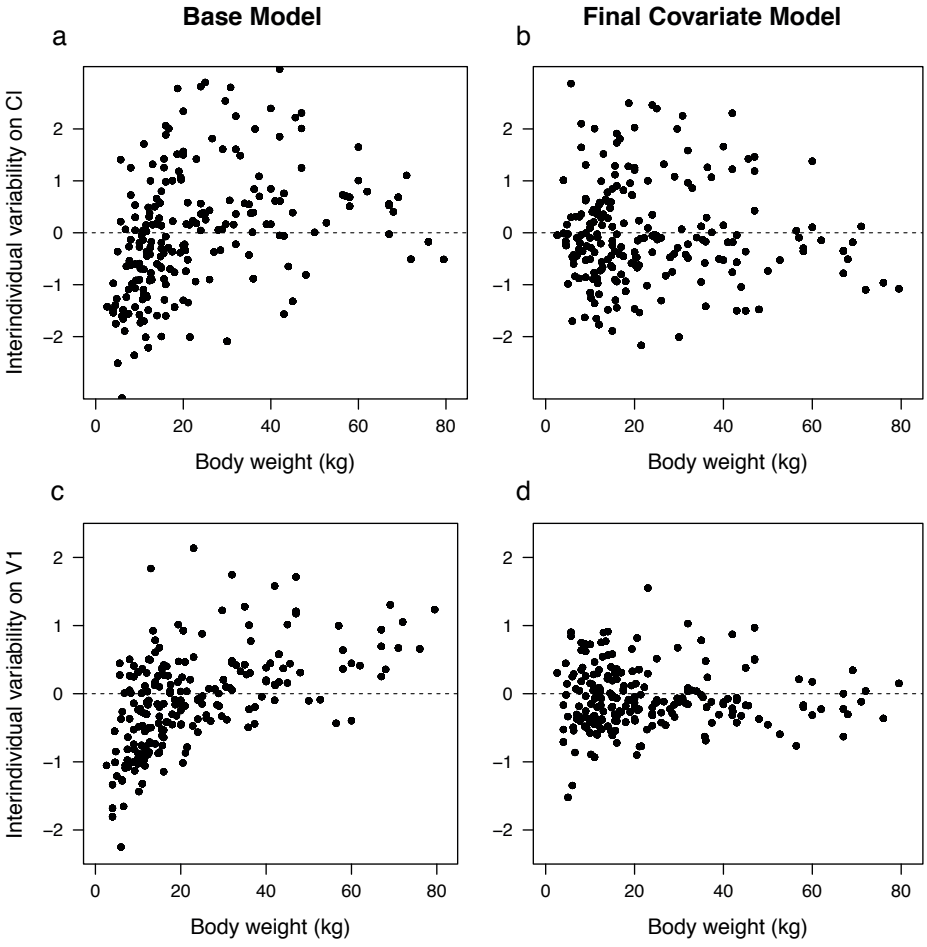

Figure 3. Interindividual variability on clearance (upper plots) and central volume of distribution (lower plots), both before (left plots) and after (right plots) inclusion of body weight as a covariate.

both models resulted in a significant decrease in OFV, however the model with parallel clearance pathways was clearly superior (-39 and -99 points in OFV for only non-linear and parallel clearance with three and four additional parameters, respectively). Therefore, alemtuzumab elimination was described using linear clearance (CL) and non-linear clearance, which was parameterized using the quotient of maximum elimination rate V_{max} and Michaelis-Menten constant K_m, depicting the concentration at which the elimination rate was 50% of Vmax. Besides a decrease of 99 points in OFV (four additional parameters, $p<0.001$), the addition of non-linear clearance to the linear clearance model resulted in an improvement in GOF-plots. The Michaelis-Menten constant could be well estimated and fell within the observed concentration range (Figure 1). No improvement of the model in

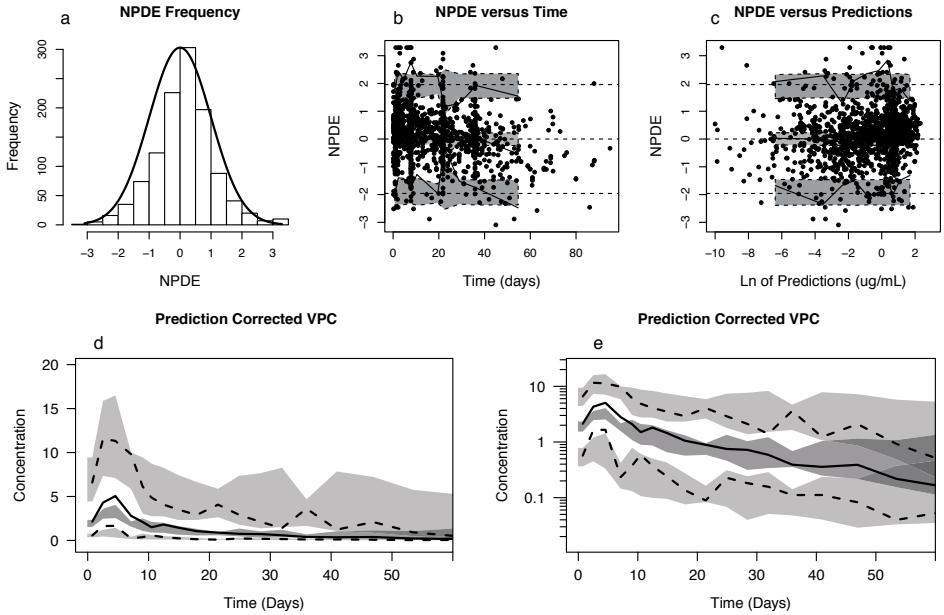

Figure 4. Validation studies. Panels A-C: Normalized Prediction Distribution of Errors (NPDE). Panel A: Histogram of the NPDE with the solid line representing a normal distribution with a mean of 0 and variance of 1. Panel B: NPDE versus time; Panel C: NPDE versus predictions. Grey blocks: 95% confidence interval of NPDE. Panels D-E: Prediction corrected visual predictive check (VPC) on a normal axis (panel D) and logarithmically transformed axis (panel E). Solid line: median of data, dashed lines: 95% confidence intervals of data, dark grey blocks: median of simulations, light grey blocks: 95% confidence intervals of simulations.

terms of OFV and goodness-of-fit-plots was observed when including IOV on any of the parameters.

Covariate Model

According to the predefined criteria, the covariate analysis showed that actual body weight and age were correlated with both central volume of distribution and linear clearance. Actual body weight proved the best predictor for both parameters both in terms of decrease in OFV and improvement of GOF plots (Figure 3). Inclusion of body weight as a power function (eq. 4) on V1 and CL yielded a decrease in OFV of 92 and 43 points, respectively. In addition, the effect of body weight on CL was parameterized as a body-weight dependent exponent (BDE), in which the exponent (k in eq. 4) differs according to body weight (Figure 3)[28,29]. Including a BDE parameterization on clearance gave a better description of the relation with body weight, especially in the smaller children, as seen in plots of interindividual variability on CL versus body weight. The exponent in this model varied from 1.94 in children of 5 kg bodyweight to 0.54 in patients weighing 80 kg. Inclusion of

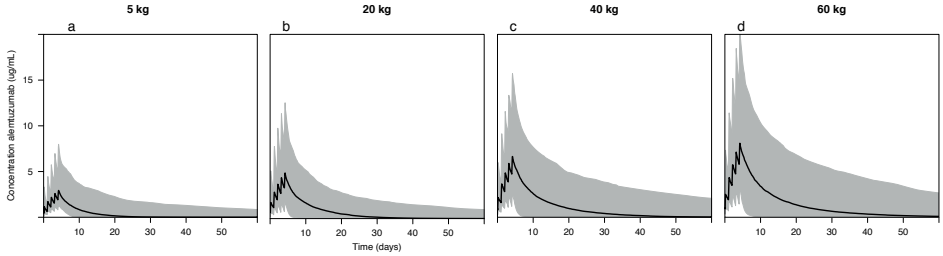

Figure 5. Simulation studies showing median (lines) and 75% confidence intervals (grey areas) of concentration over time after a cumulative dose of 1 mg/kg divided over 5 consecutive days (5 x 0.2 mg/kg/day).

a BDE-parameterization gave an additional decrease of 9 points in OFV (one additional parameter) as compared to a non-changing exponent.

Next, lymphocyte counts were evaluated as a covariate for alemtuzumab elimination. Data on lymphocyte counts were missing in 56 patients, these were set at median to give a gross covariate value of 1. Baseline peripheral blood lymphocyte counts did not influence any PK-parameter, including linear and non-linear elimination.

Internal validation

The final model with body weight on volume of distribution and in a BDE-parameterization on linear clearance was stable in bootstrap analysis (99.1% successful). The bootstrap was stratified on treatment center to account for the density of sampling. Median and 95% confidence intervals were in line with the model estimations and residual standard errors (Table 2). The NPDE-analysis showed normally distributed errors, with no major trends in NPDE versus time or NPDE versus predictions. The prediction corrected VPC shows model simulations to be well in line with model predictions, both in high and low concentrations (Figure 4).

Simulations

Concentrations over time profiles were simulated for patients with a body weight of 5, 20, 40 and 60 kg; medians as well as 95% confidence intervals are shown (Figure 5). Simulation studies show that, while using the same cumulative mg/kg dose, alemtuzumab exposure increases, proving the current dosing regimen to be suboptimal. Additionally, the unexplained variability in alemtuzumab pharmacokinetics is substantial, as seen in the confidence intervals.

DISCUSSION

Alemtuzumab plays an important role in preventing GvHD and relapse following pediatric HCT as well as the occurrence of early T-cell immune reconstitution. In this large cohort of children, we describe the population pharmacokinetics of alemtuzumab in a HCT setting. The proposed model adequately describes the observed concentrations, and was extensively validated. Actual body weight was found to be a predictor for clearance and central volume of distribution, and should therefore be taken into account for dosing of alemtuzumab. The most frequently used dosing regimen is shown to lead to escalating exposure with increasing body weight, of which the implications are yet unknown.

In the developed model, alemtuzumab elimination was best described using a parallel linear and saturable clearance pathway. This is in line with antibody pharmacology, where both target binding and non-specific degradation are the major elimination pathways. The implemented parameterization with Michaelis-Menten kinetics is often used, and particularly when the antibody targets a non-soluble protein[32]. As lymphocytes harbor the vast majority of CD52, the lymphocyte count was considered as a covariate for elimination. However, no impact of lymphocyte counts on any PK parameter was found. A possible explanation could be that a vast excess of drug is introduced in relation to the amount of CD52, thereby minimizing the effect of target availability. This should, however, be kept in mind when significantly decreasing the administered dose, as lymphocyte counts are known to influence alemtuzumab clearance at lower dosages.

One previous study by Mould et al. described the population pharmacokinetics of alemtuzumab in a population of adults treated for chronic lymphatic leukemia (CLL)[10]. Here, alemtuzumab PK was described using a two-compartment model, incorporating saturable clearance. White blood cell (WBC) count on V_{max} was found to be the only covariate predicting PK, indicating a higher maximal clearance rate in patients harboring more targets for alemtuzumab. Although the population and treatment setting in the current study is significantly different, our parameter estimates in terms of total clearance and central volume of distribution are roughly in line with their results. Importantly, the doses used in the present study (0.5-1 mg/kg) are significantly higher than those in the CLL-study, where the majority of patients received a dose of 3-30 mg (corresponding with 0.04 to 0.4 mg/kg bases on a 70-kg weighing adult). This may explain why the CLL-study did indeed find cell counts to impact elimination, while in an HCT-setting, using high doses of alemtuzumab; the role of cell counts on the PK is minor.

Few studies have investigated the dose-effect or exposure-effect relationship of alemtuzumab in terms of immune reconstitution. Nonetheless, T-cell reconstitution, especially of CD3+

and CD4+ T-cells, is suggested to be slower following higher exposures of alemtuzumab[4,6,35]. In terms of clinical outcome parameters, higher doses of alemtuzumab have been associated with a lower incidence of GvHD[1,2,4,7,9,36,37]. In one study investigating alemtuzumab concentration rather than dosage, those patients with higher concentrations on the day of HCT had less acute GvHD, but more mixed chimerism and poor immune reconstitution, however no impact on survival was demonstrated based on the concentrations on the day of HCT. The authors suggest an optimal day 0 concentration of 0.2-0.4 mcg/mL, however the simulation studies show that a majority of patients will have higher day 0 concentrations when a cumulative dose of 1 mg/kg (Figure 5).

The available evidence for the therapeutic window of alemtuzumab is still minor, and fully based on single concentrations as a predictor for outcome. Using the presented PK-model, full concentration-time profiles can be estimated for all included patients, after which multiple alemtuzumab exposure measures can be related to outcome. In previous work on the polyclonal anti-thymocyte globulin in pediatric HCT, exposure before and after HCT was found to be a powerful predictor for outcome[18]. These exposure measures may be more predictive for outcome compared to single concentrations on day 0. Following the determination of the therapeutic window, the proposed model may serve a basis for individualized dosing of alemtuzumab to ensure optimal outcome.

Besides alemtuzumab, ATG is a drug that is frequently used as serotherapy in HCT. Comparative studies between ATG and alemtuzumab show patients treated with alemtuzumab to have significantly slower immune reconstitution compared to ATG[35]. Still, alemtuzumab is associated with a lower incidence of acute and chronic GvHD when compared to ATG[38,39] but not with survival[38–41]. Albeit most centers prefer ATG over alemtuzumab, there still is a place for alemtuzumab in the conditioning of second transplants due to the possibility of anti-drug-antibody development after receiving a course of rabbit-derived ATG.

In recent years, alemtuzumab (marketed as Lemtrada®) was introduced as a treatment modality for relapsing-remitting multiple sclerosis (RRMS), where it is superior when compared to standard treatment with interferon-β in terms of relapse and disease progression[42–44]. In order to expand the economical market value for the indication RRMS, alemtuzumab was withdrawn from the market for all other indications by the manufacturer, including the brand Campath® which was registered for the treatment of CLL, prevention and treatment of solid organ transplant rejection, and as serotherapy in HCT. However, the manufacturer still has a compassionate use program for Campath making it available for use in HCT.

CONCLUSION

We have developed and extensively validated a population pharmacokinetic model, which adequately describes alemtuzumab PK over the entire pediatric age range. This model incorporates parallel linear and non-linear elimination pathways, reflecting TMDD as frequently observed in antibody kinetics. Actual body weight was identified as a covariate on clearance and volume of distribution, the former as a bodyweight-dependent exponent. Although CD52 is mainly expressed on lymphocytes, no relationship between lymphocyte counts and alemtuzumab elimination was found. Evaluation of the current dosing regimen showed that exposure varies across age and is therefore suboptimal.

This model can be used for further studies to investigate optimal alemtuzumab exposure, and subsequently serve as the basis for an individualized dosing regimen for children receiving a HCT. Using this regimen, optimal alemtuzumab exposure can be achieved, potentially improving clinical outcome in these children.

REFERENCES

1. Perez-Simon JA, Kottaridis PD, Martino R, et al. Nonmyeloablative transplantation with or without alemtuzumab: Comparison between 2 prospective studies in patients with lymphoproliferative disorders. *Blood*. 2002;100(9):3121-3127.
2. van Besien K, Kunavakkam R, Rondon G, et al. Fludarabine-Melphalan Conditioning for AML and MDS: Alemtuzumab Reduces Acute and Chronic GVHD without Affecting Long-Term Outcomes. B*iol Blood Marrow Transplant*. 2009;15(5):610-617.
3. Poire X, van Besien K. Alemtuzumab in allogeneic hematopoetic stem cell transplantation. *Expert Opin Biol Ther*. 2011;11(8):1099-1111.
4. Marsh RA, Lane A, Mehta PA, et al. Alemtuzumab levels impact acute GVHD, mixed chimerism, and lymphocyte recovery following alemtuzumab, fludarabine, and melphalan RIC HCT. *Blood*. 2015;127(4):503-513.
5. Spyridonidis A, Liga M, Triantafyllou E, et al. Pharmacokinetics and clinical activity of very low-dose alemtuzumab in transplantation for acute leukemia. *Bone Marrow Transplant*. 2011;46(10):1363-1368.
6. Lane JP, Evans PT, Nademi Z, et al. Low-dose serotherapy improves early immune reconstitution after cord blood transplantation for primary immunodeficiencies. *Biol Blood Marrow Transpl*. 2014;20(2):243-249.
7. Chakraverty R, Orti G. alemtuzumab dose before reduced intensity conditioning and HLA-identical sibling stem cell transplantation: pharmacokinetics, GVHD, and immune reconstitution. *Blood*. 2010;116(16):3080-3088.
8. Cook G, Smith GM, Kirkland K, et al. Outcome following reduced-intensity allogeneic stem cell transplantation (RIC AlloSCT) for relapsed and refractory mantle cell lymphoma (MCL): A study of the British society for blood and marrow transplantation. *Biol Blood Marrow Transplant*. 2010;16(10):1419-1427.
9. Malladi RK, Peniket AJ, Littlewood TJ, et al. Alemtuzumab markedly reduces chronic GVHD without affecting overall survival in reduced-intensity conditioning sibling allo-SCT for adults with AML. *Bone Marrow Transpl*. 2009;43(9):709-715.
10. Mould DR, Baumann A, Kuhlmann J, et al. Population pharmacokinetics-pharmacodynamics of alemtuzumab (Campath) in patients with chronic lymphocytic leukaemia and its link to treatment response. *Br J Clin Pharmacol*. 2007;64(3):278-291.
11. Elter T, Molnar I, Kuhlmann J, Hallek M, Wendtner C. Pharmacokinetics of alemtuzumab and the relevance in clinical practice. *Leuk Lymphoma*. 2008;49(12):2256-2262.
12. Rebello P, Cwynarski K, Varughese M, Eades a, Apperley JF, Hale G. Pharmacokinetics of CAMPATH-1H in BMT patients. *Cytotherapy*. 2001;3(4):261-267.
13. Morris EC, Rebello P, Thomson KJ, et al. Pharmacokinetics of alemtuzumab used for in vivo and in vitro T-cell depletion in allogeneic transplantations: Relevance for early adoptive immunotherapy and infectious complications. *Blood*. 2003;102(1):404-406.
14. Gill KL, Machavaram KK, Rose RH, Chetty M. Potential Sources of Inter-Subject Variability in Monoclonal Antibody Pharmacokinetics. *Clin Pharmacokinet*. 2016.
15. Keizer RJ, Huitema ADR, Schellens JHM, Beijnen JH. Clinical pharmacokinetics of therapeutic monoclonal antibodies. *Clin Pharmacokinet*. 2010;49(8):493-507.
16. Admiraal R, van Kesteren C, Boelens JJ, Bredius RGM, Tibboel D, Knibbe C a J. Towards evidence-based dosing regimens in children on the basis of population pharmacokinetic pharmacodynamic modelling. *Arch Dis Child*. 2014;99(3):267-272.

17. Knibbe CAJ, Danhof M. Individualized dosing regimens in children based on population PKPD modelling: are we ready for it? *Int J Pharm*. 2011;415(1-2):9-14.
18. Admiraal R, van Kesteren C, Jol-van Der Zijde CM, et al. Association between anti-thymocyte globulin exposure and CD4+ immune reconstitution in paediatric haematopoietic cell transplantation: a multicentre , retrospective pharmacodynamic cohort analysis. *Lancet Haematol*. 2015;2(5):e194-e203.
19. Yang J, Zhao H, Garnett C, et al. The combination of exposure-response and case-control analyses in regulatory decision making. *J Clin Pharmacol*. 2013;53(2):160-166.
20. Chiu Y-L, Rubin DT, Vermeire S, et al. Serum adalimumab concentration and clinical remission in patients with Crohn's disease. *Inflamm Bowel Dis*. 2013;19(6):1112-1122.
21. Wierda WG, Kipps TJ, Keating MJ, et al. Self-administered, subcutaneous alemtuzumab to treat residual disease in patients with chronic lymphocytic leukemia. *Cancer*. 2011;117(1):116-124.
22. Mould DR, D'Haens G, Upton RN. Clinical Decision Support Tools: The Evolution of a Revolution. *Clin Pharmacol Ther*. 2016;66(5):732-740.
23. Oude Munnink T, Henstra M, Segerink L, Movig K, Brummelhuis-Visser P. Therapeutic Drug Monitoring of Monoclonal Antibodies in Inflammatory and Malignant Disease – Translating TNF-α Experience to Oncology. *Clin Pharmacol Ther*. 2015;99(4):1-23.
24. Rebello P, Hale G. Pharmacokinetics of CAMPATH-1H: assay development and validation. *J Immunol Methods*. 2002;260(1-2):285-302.
25. Jol-van der Zijde C, Bredius R, Jansen-Hoogendijk A, et al. IgG antibodies to ATG early after pediatric hematopoietic SCT increase the risk of acute GVHD. *Bone Marrow Transplant*. 2012;47(3):360-368.
26. Beal SL. Ways to fit a PK model with some data below the quantification limit. *J Pharmacokinet Pharmacodyn*. 2001;28(5):481-504.
27. Wang C, Peeters M, Allegaert K, et al. A bodyweight-dependent allometric exponent for scaling clearance across the human life-span. *Pharm Res*. 2012;29(6):1570-1581.
28. Bartelink IH, Boelens JJ, Bredius RGM, et al. Body weight-dependent pharmacokinetics of busulfan in paediatric haematopoietic stem cell transplantation patients: towards individualized dosing. *Clin Pharmacokinet*. 2012;51(5):331-345.
29. Ince I, De Wildt SN, Wang C, et al. A novel maturation function for clearance of the cytochrome P450 3A substrate midazolam from preterm neonates to adults. *Clin Pharmacokinet*. 2013;52(7):555-565.
30. Krekels EHJ, van Hasselt JGC, Tibboel D, Danhof M, Knibbe C a J. Systematic evaluation of the descriptive and predictive performance of paediatric morphine population models. *Pharm Res*. 2011;28(4):797-811.
31. Comets E, Brendel K, Mentré F. Computing normalised prediction distribution errors to evaluate nonlinear mixed-effect models: the npde add-on package for R. *Comput Methods Programs Biomed*. 2008;90(2):154-166.
32. Yan X, Mager DE, Krzyzanski W. Selection between Michaelis-Menten and target-mediated drug disposition pharmacokinetic models. *J Pharmacokinet* Pharmacodyn. 2010;37(1):25-47.
33. Gibiansky L, Gibiansky E, Kakkar T, Ma P. Approximations of the target-mediated drug disposition model and identifiability of model parameters. *J Pharmacokinet Pharmacodyn*. 2008;35(5):573-591.
34. Mager DE, Jusko WJ. General Pharmacokinetic Model for Drugs Exhibiting Target-Mediated Drug Disposition. *J Pharmacokinet Pharmacodyn*. 2001;28(6):507-532.
35. Willemsen L, Jol-van der Zijde CM, Admiraal R, et al. Impact of Serotherapy on Immune Reconstitution and Survival Outcomes After Stem Cell Transplantations in Children: Thymoglobulin Versus Alemtuzumab. *Biol Blood Marrow Transplant*. 2015;21(3):473-482.

36. Lane JP, Evans PTG, Nademi Z, et al. Low-dose serotherapy improves early immune reconstitution after cord blood transplantation for primary immunodeficiencies. *Biol Blood Marrow Transplant*. 2014;20(2):243-249.
37. Peggs KS, Sureda A, Qian W, et al. Reduced-intensity conditioning for allogeneic haematopoietic stem cell transplantation in relapsed and refractory Hodgkin lymphoma: Impact of alemtuzumab and donor lymphocyte infusions on long-term outcomes. *Br J Haematol*. 2007;139(1):70-80.
38. Veys P, Wynn RF, Ahn KW, et al. Impact of immune modulation with in vivo T cell depletion and myleoablative total body irradiation conditioning regimen on outcomes after unrelated donor transplantation for acute lymphoblastic leukemia in children. *Blood*. 2012;119(25):6155-6162.
39. Soiffer RJ, Lerademacher J, Ho V, et al. Impact of immune modulation with anti – T-cell antibodies on the outcome of reduced-intensity allogeneic hematopoietic stem cell transplantation for hematologic malignancies Impact of immune modulation with anti – T-cell antibodies on the outcome of reduc. *Blood*. 2011;117(25):6963-6970.
40. Marsh JC, Pearce RM, Koh MBC, et al. Retrospective study of alemtuzumab vs ATG-based conditioning without irradiation for unrelated and matched sibling donor transplants in acquired severe aplastic anemia: a study from the British Society for Blood and Marrow Transplantation. *Bone Marrow Transplant*. 2014;49(1):42-48.
41. Park SH, Choi S-M, Lee D-G, et al. Infectious complications associated with alemtuzumab use for allogeneic hematopoietic stem cell transplantation: comparison with anti-thymocyte globulin. *Transpl Infect Dis*. 2009;11(5):413-423.
42. Coles A, Compston A, Selmaj K, et al. Alemtuzumab vs. Interferon Beta-1a in Early Multiple Sclerosis. *New Engl J Med*. 2008;359(17):1786-1801.
43. Coles AJ, Twyman CL, Arnold DL, et al. Alemtuzumab for patients with relapsing multiple sclerosis after disease-modifying therapy: A randomised controlled phase 3 trial. *Lancet*. 2012;380(9856):1829-1839.
44. Cohen JA, Coles AJ, Arnold DL, et al. Alemtuzumab versus interferon beta 1a as first-line treatment for patients with relapsing-remitting multiple sclerosis: A randomised controlled phase 3 trial. *Lancet*. 2012;380(9856):1819-1828.